Limit Sets for Once Punctured Torus Groups Acting Discretely on the Riemann Sphere

Marcel Stoklasa

Supervisor:
Prof. Dr. Maria Beatrice Pozzetti
Second Supervisor:
Dr. Gabriele Viaggi

Bachelor Thesis

Faculty of Mathematics and Computer Science
University Heidelberg
April 10th, 2022

Contents

Chapter 1

Abstract

This thesis will study the dynamics of once punctured torus groups. These groups are discrete subgroups of $PSL_2(\mathbb{C})$ and act on the Riemann's sphere via Mobius transformations.
The thesis is divided into two parts. In the first part, we construct the once punctured torus groups in $PSL_2(\mathbb{R})$ and classify them. The classification is made on the basis of the behavior of the limit set. We will prove that each group belongs to exactly one of the two classes: complete or incomplete.
In the second part, we want to deform the complete once punctured torus groups in $PSL_2(\mathbb{C})$ by two different types of deformations. They correspond to very different behaviors. The main goal here is to examine which properties of the once punctured torus groups are lost and which are preserved under which type of deformation. Consequently, we will study these deformed groups experimentally and qualitatively.

In dieser Thesis wird die Dynamik von einmal punktierten Torusgruppen untersucht. Diese Gruppen sind diskrete Untergruppen von $PSL_2(\mathbb{R})$ und wirken auf die Riemannsche Zahlenkugel durch Mobius Transformationen.
Die Arbeit ist in zwei Abschnitte eingeteilt. Im ersten konstruieren wir die einmal punktierten Torusgruppen und klassifizieren sie. Die Klassifizierung erfolgt auf der Grundlage des Verhaltens der Grenzwertmenge. Wir werden beweisen, dass jede Gruppe zu genau einer der beiden Klassen, vollstandig oder unvollstandig, gehort.
Im zweiten Teil wollen wir die vollstandigen einmal punktierten Torusgruppen in $PSL_2(\mathbb{C})$ durch zwei verschiedene Arten von Verformungen deformieren. Sie entsprechen sehr unterschiedlichen Verhaltensweisen. Das Hauptziel ist es zu untersuchen, welche Eigenschaften der einmal punktierten Torusgruppen bei den verschiedenen Deformationen verloren gehen und welche erhalten bleiben. Daher werden wir diese deformierten Gruppen experimentell und qualitativ untersuchen.

Chapter 2

Introduction

The problem we want to study in this thesis is strongly linked with 1-dimensional complex dynamics, that is, the study of iteration of holomorphic functions on the Riemann sphere $\mathbb{C} [\{\infty\}$ (see Milnor [Mil06]). We will iteratively apply holomorphic functions and examine the behavior of orbits of points as the number of iterations tends to in nity. However, the functions we will use, which are Mobius transformations, namely

$$z \mapsto \frac{az+b}{cz+d}; \text{ with } \begin{pmatrix} a & b \\ c & d \end{pmatrix} \in \mathrm{PSL}_2(\mathbb{C});$$

would not produce particularly exciting results if we restricted ourselves to only one function, which is the norm in complex dynamics.
This stems from the fact that Mobius transformations can be reduced to three basic operations: rotations, translations, and homotheties. Therefore, by iterating them, the results would be fairly predictable. Nevertheless, allowing ourselves to use two Mobius transformations A and B, or rather four transformations, since it is now reasonable to incorporate the inverse functions A^{-1} and B^{-1} as well, produces rich dynamics and a variety of interesting phenomena.
Now that we have discussed how we want to employ these functions, the question arises as to which of these Mobius transformations to choose. Our choice has a geometric nature. We consider hyperbolic once punctured torus groups, which we now brie y introduce: In the Euclidean setting, one can construct a at torus by identifying the opposite sides of a given rectangle using a pair of isometries. The shape of the torus changes geometrically as we vary the shape of the rectangle.
We can do something similar in a hyperbolic setting. One can construct a hyperbolic once punctured torus, which is a torus from which one point has been removed, by isometrically gluing the opposite sides of an ideal quadrilateral in the hyperbolic plane $\mathbb{H}^2$. As the isometries of $\mathbb{H}^2$ are naturally Mobius transformations, the identi cations of the opposite sides generate a group of Mobius transformations. We call such a group a once punctured torus group.
In the course of the thesis, we will realize that these ideal quadrilaterals can be

characterized by one value $d \in \mathbb{R}$. Due to the fact that the edges of an ideal quadrilateral have in nite length, we have one additional degree of freedom in each identi cation of opposite sides, which can be expressed with two additional parameters $s, t \in \mathbb{R}$.
Fixing these three variables, we are able to create a pair of Mobius transformations $A_{d,t}$ and $B_{d,s}$ with the geometric properties described above. We will generate a group G with these two functions whose elements are all nite compositions of the two Mobius transformations and their inverses. These groups have additional properties: They are discrete and isomorphic to a free group on 2-generators, which is the statement of the following proposition.

Proposition (Discreteness). *For every $d, t, s \in \mathbb{R}$, the group G generated by $A_{d,t}$ and $B_{d,s}$ is discrete and isomorphic to a free group on 2-generators.*

A discrete group of Mobius transformations of $PSL_2(\mathbb{C})$ is called a Kleinian group. The theory of Kleinian groups has several connections with hyperbolic geometry in dimensions 2 and 3 (see Marden [Mar07]).
The iterations we described at the beginning can be represented by G as a sequence of group elements for which we can reasonably introduce a limit. Evaluating such a limit function at any point produces a limit point, which is an element of the Riemann sphere. The collection of all possible limit points for a given group is called the limit set .
The main theorem of this thesis, which is stated below, shows a dichotomy for in terms of a linear expression involving the three parameters d, t and s: The limit sets are either circles or Cantor sets.

Theorem (Classi cation). *Given a quadrilateral Q by the parameter $d \in \mathbb{R}$ and parameters $s, t \in \mathbb{R}$, consider the once punctured torus group $G < PSL_2(\mathbb{R})$, which is generated by $A_{d,t}$ and $B_{d,s}$. For the limit set we have the following dichotomy:*

1. *If $d + t + st \neq 0$ then is a Cantor set.*
2. *If $d + t + st = 0$ then is a circle.*

Groups of the rst class are called incomplete, and groups of the second class complete. The graphic below shows a visualization of the limit set for one example from each of the two classes.

Figure 2.1: Complete and incomplete limit sets.

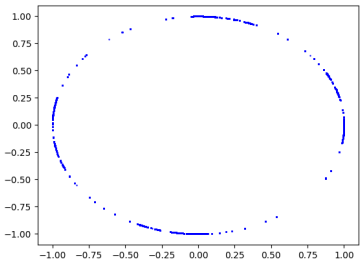

(a) Incomplete with parameters: $d \approx 0.11; t \approx 6.16; s \approx 3.3$.

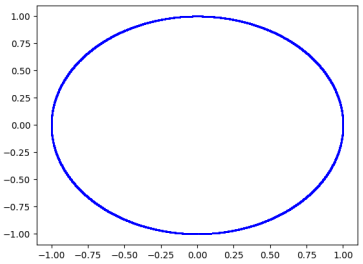

(b) Complete with parameters: $d \approx 0.11; t \approx 6.16; s \approx 6.05$.

By visualizing the limit set for several parameter combinations, we will realize that there is a correlation between $jd + t + sj$ and the size of the holes in the Cantor set, which will conclude our study of the first class.

In the second part of the thesis, we qualitatively and experimentally study several bending deformations of complete once punctured torus groups $G < PSL_2(\mathbb{R})$ in $PSL_2(\mathbb{C})$. While doing so, we will introduce three additional parameters $\quad ; \quad ; \quad 2 [\quad ; \quad)$, which describe two different types of deformations. Through experiments, we will discover that there are deformations where discreteness or being isomorphic to a free group on 2-generators is lost and others which systematically produce quasi-circles.

The following is a version of a classical theorem in Kleinian groups (as discussed for example in Chapter 5 of Outer circles [Mar07]) stated in a way that makes it convenient for us to use and is adapted to our elementary setting. The theorem provides us with a good basis to start our analysis from and gives a reason why we are excluding incomplete groups in this part of the thesis.

Theorem (Stability). *For every $d; t; s \in \mathbb{R}$, the group $G = \langle A_{d;t}; B_{d;s} \rangle < PSL_2(\mathbb{R})$ has one of the following properties:*

1. *If G is incomplete: Any small deformation $\hat{G} = \langle \hat{A}_{d;t}; \hat{B}_{d;s} \rangle < PSL_2(\mathbb{C})$ is discrete and isomorphic to a free group on 2-generators.*
2. *If G is complete: Any small deformation $\hat{G} = \langle \hat{A}_{d;t}; \hat{B}_{d;s} \rangle < PSL_2(\mathbb{C})$ with $[\hat{A}_{d;t}; \hat{B}_{d;s}] := \hat{A}_{d;t}\hat{B}_{d;s}\hat{A}_{d;t}^{-1}\hat{B}_{d;s}^{-1}$ parabolic is discrete and isomorphic to a free group on 2-generators.*

The theorem implies that incomplete groups are stable under sufficiently small deformations, whereas the complete groups are stable only under certain small deformations and can be highly unstable under other deformations. What we mean by unstable is that small changes in the parameter space lead to completely different behaviors of the limit sets, which range from nice fractals to complete chaos. The figure below shows an example of such a highly critical

scenario. In this example the limit set of the group G is a fractal, but with a slight perturbation in the parameters the limit set becomes chaotic.

Figure 2.2: Fractals and chaos.

(a) Fractal with parameters: $d = t = s = 0$ and $= =_2$.

(b) Chaos with parameters: $d = t = s = 0$ and $= 1{:}6$.

This property is again reminiscent of complex dynamics, where small alterations of the iterating function can lead to completely di erent Julia sets and slight changes of the starting parameter can turn a bounded orbit to an unbounded orbit or vice versa.
The book Indra's pearls [MSW15], in particular Chapters 6 and 8, explores similar phenomena as this thesis. They also iterate Mobius transformations and analyze the patterns this creates. However, their approach to this topic is more algebraic while ours focuses more on hyperbolic geometry.

Chapter 3

Preliminaries

This chapter provides a preliminary background on hyperbolic spaces, discrete groups, and free groups. The first section will introduce two models of the hyperbolic space and a description of its isometries. The second will describe discrete groups, limit sets, and their properties. The last will explain free groups, words, and word length.

3.1 Hyperbolic Space

Hyperbolic space and its geometry is a very broad topic, so we will only be able to scratch the surface with this introduction. For further reading, we recommend An Introduction to Geometric Topology by Bruno Martelli [Mar16], on which this section is also based.

There are several models used to describe hyperbolic space, for example the hyperboloid model, the Klein model, the half-space model and, the Poincare disk model. We will focus on the last two, but before we introduce them, we want to briefly talk about hyperbolic space in general.

Hyperbolic space, from now on denoted by $\mathbb{H}^n$, where n is the dimension, is an example of non-Euclidian geometry. It admits a well-defined notion of lines, k-dimensional planes, lengths, and angles. However, it has the property, that given an $n-1$ dimensional plane and a point, which is not part of the plane, there exist infinitely many $n-1$ dimensional planes which contain this point and are disjoint from the given plane. Nevertheless, some standard Euclidean constructions are still valid, for example, two points form a unique line and that given a line and a point there exists a unique line through the point, which is perpendicular to the given line. This concludes our general discussion, and we can move on to our first model of $\mathbb{H}^n$.

3.1.1 Poincaré Disk Model

The Poincaré disk model of H^n is the space

$$D^n := \{x \in \mathbb{R}^n \mid \|x\| < 1\},$$

endowed with lines, which are either circular arcs perpendicular to ∂D^n or straight lines through the center (see Proposition 2.1.17 in Chapter 2 [Mar16]), segments, which are parts of the unique line defined by two points, a metric, and angles.
The angles in this model are equivalent to the Euclidean ones, so we measure them as we measure the angle of intersection between two elements in Euclidean space. A model with this property is called conformal.
If n is greater than 2, then there exist infinitely many copies of D^2 inside D^n that are either disks, which are perpendicular to ∂D^n and contain the origin or S^2 spheres, which are perpendicular to ∂D^n.
Additionally, this model can be easily visualized, at least for dimensions 2 and 3, where D^n is given by the unit disk.
As we can see in Figure 3.1, we can draw hyperbolic triangles and quadrilaterals in D^2. Differently from the Euclidean case, the sum of their interior angles is smaller than 180° and 360° respectively.

Figure 3.1: Hyperbolic shapes.

(a) Hyperbolic triangle.

(b) Hyperbolic quadrilateral.

We can even go as far as creating a quadrilateral with an interior angle sum of zero. A quadrilateral with this property is called ideal, and an example can be seen in Figure 3.2. Notice the vertices of such a quadrilateral are on ∂D^2. We will assume that every quadrilateral we talk about from now on is ideal.

Figure 3.2: Ideal quadrilateral.

3.1.2 Half-Space Model

The second model we use, the half-space model

$$H^n := \{(x_1, \ldots, x_n) \in \mathbb{R}^n \mid x_n > 0\},$$

is endowed with a metric, which is again conformal to the Euclidean one. The boundary of H^n is $\mathbb{R}^{n-1} \cup \{\infty\}$. By Proposition 2.1.21 in Chapter 2 [Mar16], lines in this model are either half circles, with their centers on ∂H^n, or vertical lines. Therefore, segments exist in this model as well.
Just like in the Poincaré disk model, if n is greater than 2, there are infinitely many copies of H^2 in H^n, which are either vertical half planes or half spheres centered at a point in ∂H^n. In Figure 3.3 we can see the two ways an ideal quadrilateral can be drawn in H^2.

Figure 3.3: Quadrilaterals in the half-space model.

(a) Quadrilateral with vertices in $\mathbb{R}$. (b) Quadrilateral with vertex equal to ∞.

Before we talk about isometries we want to make one remark about distances in H^n. Obviously, distances are different in hyperbolic space compared to Euclidean space. Nevertheless, it is possible to calculate the distance between two given points in any given model with a simple formula. For our purposes, it is enough to know how to calculate the distance between two points $x, y \in H^2$,

which lie on a vertical line. For these two points the distance is given by

$$d_{H^2}(x;y) = \left|\log \frac{\mathrm{Im}(x)}{\mathrm{Im}(y)}\right| :$$

If we want a signed distance, we need an orientated line. The orientation we chose is upwards, so if x is above y, then the distance is positive, else the distance is negative. Hence, the signed distance is given by

$$_{H^2}(x;y) = \log \frac{\mathrm{Im}(x)}{\mathrm{Im}(y)} :$$

3.1.3 Isometries of H^2

The isometry group of H^2 is $PSL_2(R)$ (see Proposition 2.3.8 in Chapter 2 [Mar16]) and its elements are the projective class of 2 x 2 matrices with real entries and determinant 1, so they are invertible. $PSL_2(R)$ acts on H^2 through Möbius transformations, which we will now define.

Definition 3.1.1. The matrix $\left(\begin{smallmatrix} a & b \\ c & d \end{smallmatrix}\right) \in PSL_2(R)$ defines the following Möbius transformation

$$\begin{pmatrix} a & b \\ c & d \end{pmatrix}(z) := \frac{az+b}{cz+d}:$$

These transformations are bijective, orientation-preserving, and holomorphic. We now want to classify these transformations into three distinct types.

Proposition 3.1.1. Let $\in PSL_2(R)$ be a non-trivial isometry, then exactly one of the following holds:

1. The isometry has at least one fixed point in H^2. We call such an isometry elliptic.
2. The isometry has no fixed points in H^2 and has exactly one in $@H^2$. We call such an isometry parabolic.
3. The isometry has no fixed points in H^2 and has exactly two in $@H^2$. We call such an isometry hyperbolic.

Proof. See Proposition 2.2.5 in Chapter 2 of the book An Introduction to Geometric Topology [Mar16]. □

There is an easy way to check for a given isometry, whether it's elliptic, parabolic, or hyperbolic, by only looking at its trace.

Proposition 3.1.2. Let $\in PSL_2(\mathbb{R})$ be a non-trivial isometry, then

1. elliptic $\Leftrightarrow |\mathrm{tr}( )| < 2$,
2. parabolic $\Leftrightarrow |\mathrm{tr}( )| = 2$,
3. hyperbolic $\Leftrightarrow |\mathrm{tr}( )| > 2$.

Proof. See Proposition 2.3.9 in Chapter 2 of the book An Introduction to Geometric Topology [Mar16]. □

Every element of a given class is conjugate to the normal form of their class, which are defined as follows:

1. Elliptic transformations are conjugate to $z \mapsto \frac{\cos( )z \sin( )}{\sin( )z+\cos( )}$, with $\in [;)$.
2. Parabolic transformations are conjugate to $z \mapsto z + a$, with $a \in \mathbb{R} \setminus \{0\}$.
3. Hyperbolic transformations are conjugate to $z \mapsto z$, with $\in \mathbb{R}^+ \setminus \{1\}$.

As a consequence, every Möbius transformation is reducible to a rotation, translation, or homothety.

3.1.4 Isometries of $\mathbb{H}^3$

Before we look at the isometries, we want to introduce a representation of $\mathbb{H}^3$. We can identify $\mathbb{H}^3$ with $\mathbb{C} \times \mathbb{R}^+$ and $\partial\mathbb{H}^3$ with $\mathbb{C} \cup \{\infty\}$. So, an element of $\mathbb{H}^3$ can be written as a vector $(z;t)$, with $z \in \mathbb{C}$ and $t \in \mathbb{R}^+$, whereas an element of $\partial\mathbb{H}^3$ is just a complex number or infinity.
The isometry group of $\mathbb{H}^3$ is $PSL_2(\mathbb{C})$ (see Proposition 2.3.10 in Chapter 2 [Mar16]), which acts nicely on the boundary of $\mathbb{H}^3$ via Möbius transformation and in a more complex way on the interior.
However, if we limit ourselves to rotations R around vertical lines, the action is quite simple and given by,

$$(z;t) \mapsto (R(z);t), \text{ for every } (z;t) \in \mathbb{H}^3.$$

Hence, t is preserved and we can focus on the actions on the boundary. A rotation R^p with angle $\in [;)$ around the point $p \in \mathbb{C}$ can be written as

$$R^p(z) = (z \quad p)e^{i} + p = \frac{z \quad e^{i} + p(1 \quad e^{i})}{z \quad 0 + 1},$$

for every point $z \in \mathbb{C}$. This can then be transformed into a Möbius transformation given by the matrix

$$\begin{pmatrix} e^{i} & p(1 \quad e^{i}) \\ 0 & 1 \end{pmatrix}.$$

If we now multiply the matrix by $e^{\frac{i}{2}}$ we can change its determinant to 1. The result of this multiplication is the following matrix,

$$R^p := \begin{pmatrix} e^{\frac{i}{2}} & p(e^{\frac{i}{2}} - e^{\frac{i}{2}}) \\ 0 & e^{\frac{i}{2}} \end{pmatrix} :$$

There is an analog to Proposition 3.1.2 for the elements of $PSL_2(C)$, which is as follows:

Proposition 3.1.3. Let $2 PSL_2(C)$ be a non-trivial isometry, then

1. elliptic () $\mathrm{tr}( ) 2 (2; 2)$,
2. parabolic () $\mathrm{tr}( ) = 2$,
3. hyperbolic () $\mathrm{tr}( ) 62[2; 2]$.

For the elements in $PSL_2(C)$, there is also a normal form to which they are conjugated. These normal forms are listed below:

1. Elliptic transformations are conjugate to $z 7! e^{j} z$, with $2 [;)$.
2. Parabolic transformations are conjugate to $z 7! z + a$, with $a 2 C n f0g$.
3. Hyperbolic transformations are conjugate to $z 7! z$, with $2 C n f1g$ and $j j$ 6= 1.

3.2 Discrete Groups

In this section, which draws inspiration from Chapter 2 of the book Outer circles by Albert Marden [Mar07], we want to have a closer look at groups of Möbius transformations, precisely the ones generated by two elements. Therefore, we want to introduce a notation: First, if A and B are Möbius transformations, then we denote by $hA; B i$ the group they generate, it contains every nite composition of the four elements $A; A^{1}; B$ and B^{1}. Second, we will use $[A; B] := ABA^{1}B^{1}$, to denote the commutator of A and B.
Now we can formally de ne discreteness and the limit set for such a group.

De nition 3.2.1. A group of Möbius transformations is discrete if there is no in nite sequence of distinct elements in the group that converge to the identity.

De nition 3.2.2. For $n 2 f 2; 3g$, a point $2 @H^n$ is a limit point of the discrete group G if there exist $2 H^n [@H^n$ and a sequence of distinct elements $fT_k g 2 G$ such that $\lim_{k!1} T_k( ) = $. The set $:= f 2 @H^n j$ is a limit point g is called the limit set of G.

Remark. The limit set is, by construction invariant under G.

A discrete group is elementary if contains less than three elements. Even though the limit set can be very complicated, it always has some general properties which we will heavily use throughout the thesis.

Lemma 3.2.1 (Properties of the limit set). Suppose G is non-elementary and $n \in \{2, 3\}$.

1. The G-orbit of any $\in$ is dense in .
2. is a closed set.
3. The G-orbit of any point $x \in H^n \cup \partial H^n$ accumulates onto .
4. is a perfect set.
5. Either $= \partial H^n$ or its interior is empty.

Proof. See Lemma 2.4.1 in Chapter 2 of the book Outer circles [Mar07]. □

Lastly, we will define Cantor spaces and relate them to the standard Cantor set.

Definition 3.2.3. A space is a Cantor space if it is compact, metrizable, perfect, and totally disconnected.

The following lemma will be stated without a proof, because it is a known topological fact.

Lemma 3.2.2. Every Cantor space is homeomorphic to the standard Cantor set.

3.3 Free Groups

For later chapters it will be of occasional use to be familiar with free groups, words, and reduced word length. But these definitions will come up mainly in remarks or sidenotes, so this introduction will only be superficial. For more details, refer to Office Hours with a Geometric Group Theorist [CM17].
We will start by defining a word on a set of letters. In our case, this set will only contain A and B, but even an infinite set would be possible. A word is then given as a finite string consisting of these letters and the inverses of these letters, for example:

$$AB; \quad A\,{}^{1}BBBAA\,{}^{1}; \quad BAA\,{}^{1}BB\,{}^{1}B\,{}^{1}A:$$

The empty word, which is a string containing no letters, is also a legal word.
In contrast to a word, a reduced word is one where the letter A is never next to A^{-1} and B is never next to B^{-1}. As the name suggests, we can always take a word and reduce it. This is achieved by eliminating every instance of such an occurrence. If we take the last word from our previous example, it can be reduced as follows:

$$BAA\,{}^{1}BB\,{}^{1}B\,{}^{1}A \;7!\; BBB\,{}^{1}B\,{}^{1}A \;7!\; BB\,{}^{1}A \;7!\; A:$$

We have done the reduction from left to right, but the sequence actually does not matter, the result is always the same.
The (reduced) word length is given as the number of letters in the reduced representation of a word, so the word from our last example has a word length of 1.
With this, we are able to formally de ne a free group on 2-generators and link it to the groups of Mobius transformations.

De nition 3.3.1. The free group of 2-generators is the group

$$F_2 := \{\text{reduced words in } A \text{ and } B\}$$

with the multiplication: concatenate, then reduce. We can create the inverse of a group element by swapping each letter with its inverse and arranging the word in reverse order.

Remark. For a given group G and every $g_A, g_B \in G$, there exists a unique group homomorphism between F_2 and G, such that $(A) = g_A$ and $(B) = g_A$.

We can show, via the following lemma, that a given group is isomorphic to a free group of 2-generators.

Lemma 3.3.1 (Ping-Pong). Suppose A and B generate a group G that acts on a set X. If

1. X_A, X_B X are disjoint nonempty subsets, and
2. $A^k(X_B)$ X_A and $B^k(X_A)$ X_B for all non-zero powers k,

then G is isomorphic to a free group of 2-generators.

Proof. See Lemma 5.1 in Chapter 5 of O ce Hours with a Geometric Group Theorist [CM17]. □

If a group $G = \langle A, B \rangle < PSL_2(\mathbb{C})$ is isomorphic to a free group of 2-generator, G is a free group and in context of our groups of Mobius transformations this means that no reduced word (composition of Mobius transformations) except the empty word is equal to the identity. In addition, this provides us with a nice way to represent our group as a graph, the so-called Cayley graph. An example of such a graph can be seen in Figure 3.4 .

Figure 3.4: Cayley graph of word length 3.

Chapter 4

Dimension 2: Classification of Once Punctured Torus Limit Sets

Introduction

In this chapter we introduce the once punctured torus groups $G < PSL_2(\mathbb{R})$ and classify them in terms of the behavior of their limit sets.

Our torus groups $G = \langle A, B \rangle$ are generated by a pair of isometries A, B of H^2 that identify the opposite sides of an ideal quadrilateral Q. Because the vertices of our quadrilaterals are not elements of the hyperbolic space, the quotient $Q/A \cup B$ is a punctured torus. This motivates the terminology once punctured torus groups.

These groups G will be discrete. Hence, they have well-defined limit sets. The main result of this chapter is a classification theorem that relates the behavior of the limit sets to the quadrilateral parameter $d \in \mathbb{R}$ and the two gluing parameters $t, s \in \mathbb{R}$.

The qualitative behavior of the limit sets will only depend on a linear expression of these three parameters, which will be introduced at the beginning of this chapter.

Having proven the theorem, we will visualize the limit sets for specific parameters, verifying our findings and examining the qualitative features in regard to a number of geometric quantities.

4.1 Creating a Once Punctured Torus Group

The three parameters mentioned in the introduction of this chapter consist of one quadrilateral parameter $d \in \mathbb{R}$ and two gluing parameters $t, s \in \mathbb{R}$.
To get our quadrilateral parameter, we first want to reduce the set of quadrilaterals we have to consider. To achieve this, we recall that two quadrilaterals Q and $\tilde{Q}$ are congruent if there exists an isometry $\phi \in PSL_2(\mathbb{R})$ such that $\phi(Q) = \tilde{Q}$. Congruent quadrilaterals form equivalence classes. For our purposes, we only need one quadrilateral for every equivalence class. We have:

Lemma 4.1.1. Given a quadrilateral Q, there exists an isometry $\phi \in PSL_2(\mathbb{R})$ such that the vertices of $\phi(Q)$ are $-1, 0, e^d, 1$, with $d \in \mathbb{R}$.

Proof. We denote that an element of $PSL_2(\mathbb{R})$ will always allow us to send three points to three other points of our choosing, hence we can send three vertices of any given quadrilateral to the points $-1, 0$ and 1 in such a way that the remaining vertex has to be between 0 and 1. Therefore, we can write the remaining vertex as e^d with $d \in \mathbb{R}$. □

Remark. The parameter $d \in \mathbb{R}$ has a geometric meaning, it is the signed distance $_{\mathbb{H}^2}(ie^d, i)$ between the orthogonal projections of the vertices -1 and e^d onto the diagonal of 0 and 1 (see Figure 4.1). Since distances are preserved under isometries we can check whether this property holds for the other diagonal by sending the vertices -1 and e^d through an isometry to 0 and 1 respectively. To preserve the orientations of the lines we need to send 0 to 1 and by a simple calculation, we can show that -1 must be mapped to e^d. Therefore, the signed distances for both diagonals coincide, making d an intrinsic quantity of the quadrilateral Q.

Figure 4.1: Geometric meaning of d.

From now on, we will assume that a quadrilateral is in the form of the previous lemma.
We will now discuss the gluing parameters. Notice that given two opposite oriented sides l, l' of Q there are infinitely many isometries $\phi \in PSL_2(\mathbb{R})$ such

that $\varphi(l) = l'$. In order to parametrize them, we introduce a gluing parameter: We use perpendicular lines from the vertices of 0 and ∞ through the opposite edges. We can see in Figure 4.2 that this gives us the points $1/2 + 1/2i$ and $e^d + ie^d$ for the first identification and the points $-1 + i$ and $1/2e^d + 1/2ie^d$ for the second identification, which serve as the base points.

Figure 4.2: Orthogonal projection.

If we had determined that these points had to be identified with each other, we would have had a single pair of isometries, but we want to permit all possible identifications. Thus, we allow the points on the vertical lines to shift and keep track of their position via the signed distances $t, s \in \mathbb{R}$ from the base positions. The distance on vertical lines is logarithmic, hence the new points are precisely $-1 + ie^{-s}$ and $e^d + ie^{d+t}$. The two numbers t, s serve as our gluing parameters and with them, we can finally construct our matrices.

Proposition 4.1.2. Given $d, t, s \in \mathbb{R}$ the isometries $A_{d,t}, B_{d,s} \in PSL_2(\mathbb{R})$ with the following properties

$$A_{d,t}(0) = e^d, \quad A_{d,t}(-1) = \infty, \quad A_{d,t}(1/2 + 1/2i) = e^d + ie^{d+t},$$
$$B_{d,s}(0) = -1, \quad B_{d,s}(e^d) = \infty, \quad B_{d,s}(1/2e^d + 1/2ie^d) = -1 + ie^{-s},$$

are given by the matrices

$$A_{d,t} = \begin{pmatrix} e^{\frac{t+d}{2}} & e^{\frac{d-t}{2}} \\ e^{\frac{t+d}{2}} & e^{\frac{t+d}{2}} \end{pmatrix}, \quad B_{d,s} = \begin{pmatrix} e^{\frac{s+d}{2}} + e^{\frac{s-d}{2}} & e^{\frac{s+d}{2}} \\ e^{\frac{s-d}{2}} & e^{\frac{s+d}{2}} \end{pmatrix}.$$

Proof. This can be proven by simple computations. □

To end this section, we will have a first look at the groups created by our identifications $A_{d,t}, B_{d,s}$ and prove that for any given triple of parameters $d, t, s \in \mathbb{R}$ the group G generated by the two matrices is isomorphic to a free group on 2-generators and discrete. This proof of discreteness is necessary to talk about their limit sets.

Proposition 4.1.3. For every $d; t; s \in R$, the group G generated by $A := A_{d;t}$ and $B := B_{d;s}$ is discrete and isomorphic to a free group on 2-generators.

Proof. Suppose there exists a sequence of distinct elements $T_n \in G$ for every $n \in N$, such that T_n converges to the identity. In this case, for any given $\varepsilon > 0$ and $x \in H^2$ there exists a $N_{\varepsilon;x} \in N$, such that the distance between $T_n(x)$ and x is smaller or equal to ε.
Let o be a point in the interior of the quadrilateral Q given by the parameter $d \in R$. This point has a positive distance from every edge of the quadrilateral, let δ be the smallest of such distances. Thus, the distance between o and any other point in the complement of Q is bigger than δ. Choose ε smaller than δ and $n \in N$ bigger than the corresponding $N_{\varepsilon;o} \in N$. To finish the proof, it is now sufficient to prove that $T_n(o) \in Q^c$.
The complement of Q will be split into the four open disjoint sets $S_A; S_{A^{-1}}; S_B$ and $S_{B^{-1}}$, as in Figure 4.3.

Figure 4.3: Disjoint sets.

These open sets and the interior of Q have the following interactions with our identifications,

$$A(Q^o) \subset S_A; \quad A^{-1}(Q^o) \subset S_{A^{-1}}; \quad B(Q^o) \subset S_B; \quad B^{-1}(Q^o) \subset S_{B^{-1}}; \tag{4.1}$$

$$A(S_A \cup S_B \cup S_{B^{-1}}) \subset S_A; \quad A^{-1}(S_{A^{-1}} \setminus S_B \setminus S_{B^{-1}}) \subset S_{A^{-1}}; \tag{4.2}$$

$$B(S_B \cup S_A \cup S_{A^{-1}}) \subset S_B; \quad B^{-1}(S_{B^{-1}} \cup S_A \cup S_{A^{-1}}) \subset S_{B^{-1}}. \tag{4.3}$$

This is a direct result of our definitions and the fact that Möbius transformations are bijective, holomorphic, and orientation preserving functions.
We will now show via mathematical induction that $T_n(o) \in Q^c$. We can write $T_n = w_n w_{n-1} \cdots w_2 w_1$ with $w_i \in \{A; A^{-1}; B; B^{-1}\}$ for every $i \leq n$. The base case follows by Equation (4.1).
For the induction step, we assume that our statement holds for a given $k < n$, and, hence $T_k(o) \in Q^c$. Without loss of generality, $T_k(o) \in S_A$, because of the symmetries in Equations (4.2) and (4.3). As a consequence, we know that $w_k = A$ and $w_{k+1} \neq A^{-1}$.

From Equation (4.2), Equation (4.3), and $w_{k+1} \neq A^{-1}$ now follows that $T_{k+1}(o) \in Q^c$. This concludes the proof of discreteness.
The proof of the second statement follows directly from Equations (4.2) and (4.3) and Lemma 3.3.1. □

4.2 The Classification Theorem

The following section will consist mainly of the proof of the main theorem:

Theorem 4.2.1 (Classification). Given a quadrilateral Q by the parameter $d \in \mathbb{R}$ and gluing parameters $s, t \in \mathbb{R}$, consider the once punctured torus group $G = \langle A, B \rangle < PSL_2(\mathbb{R})$, where $A := A_{d;t}$ and $B := B_{d;s}$. For the limit set Λ we have the following dichotomy:

1. If $d + t + s \neq 0$ then $\Lambda \subsetneq \partial\mathbb{H}^2$ is homeomorphic to the Cantor set.
2. If $d + t + s = 0$ then $\Lambda = \partial\mathbb{H}^2$.

Proof. Before going into the details about the proof, we will briefly outline the strategy taken within it. To prove this theorem, we will consider the two cases separately. Both use the properties of the polygonlike set $P := \bigcup_{w \in G} w(Q)$ and the commutator $[A, B]$, which will be discussed later in the proof.
According to the lemma below, it will be sufficient to find a single element in Λ^c to prove the first case of the theorem. We will achieve this by the construction of a line, which is invariant under $[A, B]$ and disjoint from P. This will give us an open interval of $\partial\mathbb{H}^2$ that has to be contained in Λ^c concluding this case.

Lemma 4.2.2. If Λ is a proper subset of $\partial\mathbb{H}^2$, then it is homeomorphic to the Cantor set.

Proof. By Lemma 3.2.1, Λ is a closed, perfect set with empty interior. As a subset of a compact metrizable set, it is compact and metrizable. Because it has an empty interior and is closed its complement is an open set which is dense in $\partial\mathbb{H}^2$. Hence, between every two points from Λ exists an open interval in Λ^c, making Λ totally disconnected. □

To prove the second case, we will start by showing that P has to cover $\mathbb{H}^2$. Using that, we will deduce that there cannot exist an open interval of $\partial\mathbb{H}^2$ in Λ^c. By the properties of the limit set (Lemma 3.2.1), this will be sufficient to conclude the proof of the second case.
As mentioned before, preceding the proof of the first case, we will make some observations, mostly about P and the commutator $[A, B]$.

Obs. 1. If $w_1, w_2 \in G$, $w_1 \neq w_2$ then $w_1(Q^o) \cap w_2(Q^o) = \emptyset$, otherwise $w(Q^o) \cap Q^o \neq \emptyset$, where $w = w_2^{-1} w_1 \neq \mathrm{Id}$ and we have shown in Proposition 4.1.3 that this is not possible.

Obs. 2. For every $w \in G$, $w(P) = P$ and $w(\Lambda) = \Lambda$. This is a direct consequence of the definitions.

Obs. 3. P is convex. To show this, we simply need to prove that adding a quadrilateral to a convex polygon maintains the convexity. The starting quadrilateral Q and every quadrilateral we add are convex. So if we add a new quadrilateral $\hat{Q}$ to a convex polygon $\hat{P}$, by our convention, and choose one point p in our polygon and one point q from $\hat{Q}$, the line l through p and q has to cross the common edge at a point c. This point c is part of both figures, so the segments $s_{[p;c]}$ and $s_{[c;q]}$ have to be contained in their respected figures, because of their internal convexity. Therefore, the segments $s_{[p;q]}$ is contained in $\hat{P} \cup \hat{Q}$.

Obs. 4. The commutator $[A; B]$ is given by the matrix

$$\begin{pmatrix} e^{t+d+s} & (e^{-s} + e^{-s-t} + e^{d+t} + e^{d} + e^{d+t+s} + 1) \\ 0 & e^{-t-d-s} \end{pmatrix};$$

with $|\mathrm{tr}([A; B])| = e^{t+d+s} + e^{-t-d-s}$ and $\mathrm{Im}([A; B](x + iy)) = e^{2(t+d+s)}y$.

Obs. 5. The commutator $[A; B]$ has exactly one fixed point, which is ∞, if and only if $d + t + s = 0$. In that case, it is a parabolic transformation.
As a consequence, if $d + t + s \neq 0$ the commutator $[A; B]$ is a hyperbolic transformation. It has two distinct fixed points in $\partial\mathbb{H}^2$ and one of those two points has to be ∞. This is a direct result from Obs. 4.

Proof of case 1 (Λ is a Cantor set). By Obs. 5, we know that the commutator $[A; B]$ is a hyperbolic isometry that fixes ∞ and $p \neq \infty$. Consequently, the line $l_{[p;\infty]}$ is the invariant axis of $[A; B]$.
The line $l_{[p;\infty]}$ is either disjoint from P or it intersects it. Suppose there exists a $w \in G$ such that $w(Q)$ and $l_{[p;\infty]}$ intersect. There are two ways how they could intersect, the quadrilateral $w(Q)$ and $l_{[p;\infty]}$ could either have a common boundary point at ∞, as seen in Figure 4.4 or not, like in Figure 4.5.

Figure 4.4: $l_{[p;\infty]}$ and $w(Q)$ meet at ∞

Suppose $l_{[p;\infty]}$ and $w(Q)$ meet at ∞. By Obs. 4, we know that points of $l_{[p;\infty]}$ can only be shifted upwards or downwards by a fixed factor by the commutator $[A; B]$. Hence, $[A; B]w(Q^o) \cap w(Q^o) \neq \emptyset$, which is a contradiction to Obs. 1. Therefore, this is not possible.

Figure 4.5: $l_{[p;1]}$ and w(Q) cross.

Suppose $l_{[p;1]}$ and w(Q) cross. By Obs. 5, we know that p and 1 are the only fixed points of $[A;B]$. Consequently, for large $n \in \mathbb{N}$ either the vertices of $[A;B]^n w(Q)$ or the vertices of $[A;B]^{-n} w(Q)$ will tend to 1. However, $l_{[p;1]}$ has to cross the quadrilaterals for every n. Therefore, at least one vertex will tend to 1 through the positive numbers and at least one through the negative numbers. Hence, there exists a $z \in \mathbb{Z}$ such that $[A;B]^z w(Q^o) \cap Q^o \neq \emptyset$, which is again a contradiction with Obs. 1.
As a consequence $l_{[p;1]}$ is disjoint from P, $(p;1) \cap \Lambda = \emptyset$, and $p;1 \in \Lambda$. By Lemma 4.2.2, it follows that Λ is homeomorphic to the Cantor set. This concludes the first case.

Proof of case 2 ($\Lambda = \partial\mathbb{H}^2$). We will start this case with some further observations, which stem from the convexity of P (Obs. 3) and Obs. 5, which says that the commutator is a parabolic transformation if $d + t + s = 0$.

Obs. 6. The rectangle

$$R := \{z = x + iy \in \mathbb{H}^2 \mid y \quad \frac{2e^{d+t} + e^d + 1}{2}\};$$

is contained in P, this can be easily verified by realizing that the commutator acts as a horizontal translation, so the nearest vertices of two adjacent quadrilaterals always have the same distance, $2e^{d+t} + e^d + 1$. The line between these vertices is a half circle, with radius $1/2(2e^{d+t} + e^d + 1)$, and every point on or above it has to be contained in P because of convexity. The claim now follows. As P is invariant under G (Obs. 2),

$$R_G := \bigcup_{w \in G} w(R) \quad P:$$

The set R_G contains the rectangle R for the vertex of infinity and a disk for every other vertex. By our definition, the vertices are not part of this set. With this observation, we want to prove the following claim:

$$P = \mathbb{H}^2: \tag{4.4}$$

To do so, it is enough to show that P can be extended by $\varepsilon > 0$ and still be contained in P, which means that for every point $x \in P$ the open ball with radius ε is contained in P.
By the definition of P, there must exist an element $w \in G$ for every $x \in P$, such that $w(x) \in Q$. Therefore, it is sufficient to show that an ε-neighborhood of Q is contained in P.
With the set R_G and the convexity of P (Obs. 3) we see in Figure 4.6 that we can easily find such an ε for points in $Q \cap R_G$.

Figure 4.6: ε-extension of Q.

Without loss of generality, we only have to check one vertex, in this case v_1, because we can send all vertices to infinity using G.
We can shift the lower edge of the rectangle R upwards by ε, this may lead to a new smaller $\tilde{\varepsilon}$, but with the convexity argument there still has to exist one $\tilde{\varepsilon}$ bigger than zero, for every point in $(Q \setminus R) \cap R_\varepsilon$. This new rectangle R_ε is contained in R and every point in R_ε has at least a distance of ε to the boundary of R. Therefore, for every point in R_ε exists an open ball of radius which is contained in P.
In conclusion, we found an ε-neighborhood Q that is contained in P, which proves our claim.
Now suppose $\neq \partial H^2$. Then has to be a closed set with empty interior (Lemma 3.2.1), thus its complement has to be an open set which is dense in ∂H^2. Hence, there has to exist an open interval in ^{c}, with endpoints $_1, _2 \in \partial H^2$. This open interval corresponds to an open half plane, which has to intersect P (Equation (4.4)). Because P is convex, the open interval has to contain a vertex of P. However, the vertices of P are a subset of . Hence, $\cap (_1, _2) \neq \emptyset$, this contradicts with $(_1, _2) \subset ^c$. Therefore, $= \partial H^2$, which concludes the second case and the proof.

□

Now that we are done with the construction and classi cation of our torus groups, we will have a brief geometrical look at the quotient $Q=A[B$, which is a hyperbolic once punctured torus (see Figure 4.7). There are two ways a torus can be punctured: It can either miss a circle, which corresponds to the rst case of our theorem, or miss a single point at in nity, which corresponds to the second. We will call tori of the rst class incomplete and tori of the second class complete.

Figure 4.7: Once punctured tori.

(a) Incomplete structure.

(b) Complete structure.

4.3 Visualization of Limit Sets

The visualization will be done using a Python script. We can simplify the programming by recalling a fact from Lemma 3.2.1, which states that the G-orbit of any 2 is dense in . By Obs. 5, 1 is always a xed point of the commutator and thus 1 2 for every group. Therefore, it is enough to start with 1 or any other vertex of our quadrilateral Q.
There is still one problem to solve, namely, that the computational time and the required memory grow exponentially in relation to the word length. However, this is more of an inconvenience than a problem, because a comparatively small length of 14, which a normal computer is capable of handling, is enough to produce a good approximation.
Nevertheless, this is not the approach we used to create the following pictures, but it would be beyond the scope of this section to explain in detail the method we used.
One last remark before we proceed with the rst example: The calculations were done in the half plane model, but we will look at them in the Poincare disk model. This gives us the advantage of being able to see the complete boundary, so we don't miss a phenomenon that may only occur for large numbers.

Example 4.3.1. For the first set of examples we choose the parameters d, t, s at random in the parameter space $(d, t, s) \in [-10, 10]^3$. We can see in Figure 4.8, that we got two Cantor sets, which is exactly what we expected, because the sum of three random numbers is almost surely different from zero.

Figure 4.8: Random parameters.

(a) $d = 0.11, t = 6.16, s = 3.3$. (b) $d = 0.43, t = 0.25, s = 0.11$.

Example 4.3.2. In this example, we want to verify that we actually get a complete structure if we choose our parameters so that they add up to zero. The first one is the trivial example, where $d = t = s = 0$. Even though this set of parameters may seem uninteresting, they form the basis of the next chapter. The second example used d and t from Figure 4.8a and changed s to satisfy the equation.

Figure 4.9: Complete structures.

(a) $d = t = s = 0$. (b) $d = 0.11, t = 6.16, s = 6.05$.

Example 4.3.3. In the last example, we want to have a closer look at incomplete structures. We want to see if there is a link between the parameters we choose and how large the gaps in are. As a reference, we use Figure 4.8b and de ne a new parameter $l := d + t + s$, which is approximately 0:79 in this case. The following gures are obtained by rescaling $d; t$ and s by $1;\ 1; 1=3; 3$.
On the one hand, Figure 4.10b indicates, that changing the sign does not change the size of the gaps, it only ips the picture horizontally. On the other hand, Figures 4.10c and 4.10d suggest that the size of the gaps correlates with the size of l. With these two observations, we conclude that the gap size depends on the absolute value of l.

Figure 4.10: Incomplete structures.

(a) l. (b) l.

(c) $1=3\,l$. (d) $3l$.

Chapter 5

Dimension 3: Bending Deformation Experiments on Complete Structures and Quasi Circles

Introduction

In this chapter, the once punctured torus groups G, which are subgroups of $PSL_2(\mathbb{R})$, will be deformed in $PSL_2(\mathbb{C})$. In order to do so, we embed Q in H^3 and add rotations to the gluing maps.
For these rotations, we will introduce three additional parameters $\ ;\ ;\ 2[\ ;\ )$, which describe two types of deformations, that correspond to very di erent behaviors. The rst angle de nes a bending of the quadrilateral Q along its diagonal of 0 and 1 . When G corresponds to $d = t = s = 0$ the groups generated with this parameter will almost always be non-discrete, the consequences of which will be discussed and experimentally explored in the rst section.
The remaining two angles and are used as gluing angles, which apply rotations to the quadrilaterals $A_{d;t}(Q)$ and $B_{d;s}(Q)$ in respect to Q. For these parameters, we will only focus on tuples where = , the resulting groups will be discrete up to a certain angle. When visualizing the limit sets for such groups, we will observe that the circles will be deformed into fractal curves. Additionally, we will search the speci c angle, where the groups stop being discrete, and explore the properties of the corresponding group.
There are obviously many possibilities left, which we unfortunately cannot study in this chapter. We could, for example, loosen our constraint on and or utilize all three parameter simultaneously, both of these options yield fascinating results.

5.1 Bent Quadrilaterals

In this section we study subgroups of $PSL_2(\mathbb{C})$ which are deformations of complete groups $G = \langle A_{d;t}; B_{d;s}\rangle$ generated by certain isometric identifications of opposite sides of bent quadrilaterals. These deformations provide examples where the property of discreteness or the property of being isomorphic to a free group on 2-generators is lost.
A bent quadrilateral $Q_{d;}$ is an object as the one shown in Figure 5.1: It is obtained by bending the standard quadrilateral $Q_d \subset \mathbb{H}^2 \subset \mathbb{H}^3$ with the vertices $1; 0; e^d$ and 1 along the diagonal $l_{[0;1]}$ by an angle .

Figure 5.1: Bending parameter .

We now discuss the identifications $A_{;d;t}$ and $B_{;d;s}$ that we are considering: We only adjust the isometries $A_{d;t}$ and $B_{d;s}$ that identify the opposite sides of the standard quadrilateral $Q_d \subset \mathbb{H}^3$ so they account for the bending. The best way for this is to apply the rotations and the identifications independently. So if we want to create $A_{;d;t}$, we start with $A_{d;t}$ and then rotate with R^0. The creation of $B_{;d;s}$ proceeds anti symmetrically, so we start with the rotation R^0_9 and then apply $B_{d;s}$. We combine these constructions in the following definition:

Definition 5.1.1. Given the parameters $d; t; s \in \mathbb{R}$ and $\in [\ ;\ )$, the isometries $A_{;d;t}; B_{;d;s} \in PSL_2(\mathbb{C})$, that identify the opposite edges of a bent quadrilateral are given by the matrices

$$A_{;d;t} = \begin{pmatrix} e^{i\frac{}{2}} & 0 \\ 0 & e^{-i\frac{}{2}} \end{pmatrix} A_{d;t}; \quad B_{;d;s} = B_{d;s} \begin{pmatrix} e^{-i\frac{}{2}} & 0 \\ 0 & e^{i\frac{}{2}} \end{pmatrix}$$

Before we head to the visualization, we want to examine, which properties from the previous chapter are lost in this setting. For this investigation we will set the parameters $d; t$ and s to 0, which motivates the following notations:

$$A := A_{;0;0}; \quad B := B_{;0;0}:$$

We will start with some observations on the commutator, which is given by the matrix

$$[A\ ;B\ ] = \begin{matrix} e^{i} & 3 & 3e^{i} \\ 0 & & e^{\ i} \end{matrix} :$$

If we exclude 0 and , which correspond to the angles that preserve the real line, the commutator is always elliptic and can be rewritten as a rotation matrix R_2^p , that describes a rotation by 2 around the point $p = \frac{3e^{i}}{e^{i} \quad 1}$.
We explore the consequences of this in the subsequent lemma.

Lemma 5.1.1. *Given 2 (;) n f0g, the commutator* $[A\ ;B\ ]$ *has the following properties:*

1. *If 2* Q *, there exists a k 2* N*, such that* $[A\ ;B\ ]^k = Id.$
2. *If 2* Q *, there exists a sequence* k_n *2* N *for every n 2* N*, such that* $[A\ ;B\ ]^{k_n} \ ! \ Id.$

Proof. If *2* Q , then 2 *2* Q . Hence, there exist *h; k 2* N, such that 2 = 2 $^{h=k}$, which is equivalent to 2 *k* = 2 *h*. Therefore, the following equation holds:

$$[A\ ;B\ ]^k = (R_2^p\ )^k = R_{2\ k}^p = R_{2\ h}^p = R_0^p \ = Id:$$

This concludes the proof of the rst statement.
If 2 Q , then 2 *k* 6= 2 *h* for every *k; h 2* N, by the preceding equation follows, $[A\ ;B\ ]^k$ 6= *Id* for every *k 2* N. Therefore, the set

$$f \ 2\ [0; 2\ )\, j \ = 2\ k\, mod(2\ ); k\ 2\ \mathrm{N}g;$$

is dense in [0; 2). So, there exists a sequence k_n *2* N for every *n 2* N, such that 2 $k_n\, mod(2\ )$! 0. Hence, the following equation holds:

$$[A\ ;B\ ]^{k_n} = (R_2^p\ )^{k_n} = R_{2\ k_n}^p \ ! \ R_0^p \ = Id:$$

□

This lemma implies that the properties of the complete groups $G < PSL_2(\mathbb{R})$ which we constructed in the previous chapter are not stable under small perturbations. If we recall the group homomorphism from F_2 to *G*, with the requirement $(A) = A$ and $(B) = B$, then it follows that the mapping is non-injective for the rst case and non-discrete for the second.
Our de nition of the limit set relied on the discreteness of the group, with this property lost for almost all , we need to further study these groups.
It would be possible to prove, that if 2 Q , the group *G* generated by *A* and *B* is dense in $PSL_2(\mathbb{C})$. However, we will skip the proof of this statement, since it relies heavily on Lie groups, which we have not introduced and would be of no further use to us. Furthermore, we mainly intend to give a sense of what we expect in the following experiments.
The consequence of this statement is, that the closure of the orbit of any point under a group *G*, which is generated by *A* and *B* , is almost always equal to the boundary of H^3. So in comparison to the last chapter, we are expecting to see vastly di erent gures, they should be signi cantly more chaotic.

Before we start with the visualization, we will brie y talk about the methods used and justify them. Foremost, we notice that we can take over a large part of the old script, we only have to change the used matrices as it is described in De nition 5.1.1. Now we can calculate the orbit of any point in $@H^3$ up to a certain word length.
In the last chapter, in order to visualize the orbit, we used the following inversion,

$$z \mapsto \frac{z+i}{iz+1};$$

that mapped $@H^2$ onto $@D^2$ or more generally $\mathbb{R} [\{ f 1 g$ onto S^1. This inversion is a so-called Mobius anti-transformation, which just like Mobius transformations preserves the Riemann sphere. The orbit of a point is a subset of the boundary of H^3 and the boundary of H^3 corresponds exactly to the Riemann sphere. Hence, the inversion above is also well-de ned for orbits of points under the deformed groups $\hat{G}$.
We end this discussion with the following observation: For small perturbations, the orbit of a point under $\hat{G}$ is still close to $\mathbb{R} [\{ f 1 g$ if we work with a limited word length. Therefore, the inversion continues to map the orbit approximately onto S^1, thus it is useful to maintain this inversion to study the e ect of the deformations.

Experiment 5.1.1. In our rst experiment (see Figure 5.2) we have chosen values near zero. The result of this is still nearly a circle only the vertices of our starting quadrilateral seem to separate themselves from the rest of the circle.
This is the opposite of what we were expecting, so we need to go troubleshooting. Some possible errors are computer inaccuracy or the limited word length. If this behavior persists for increased values of , we can rule out the rst case, which we will attempt in our second experiment.

Figure 5.2: Values near zero.

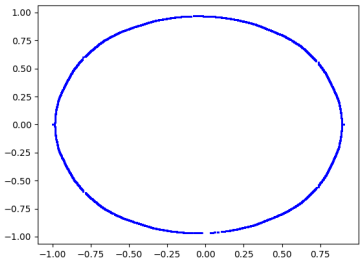

(a) = 0:1.

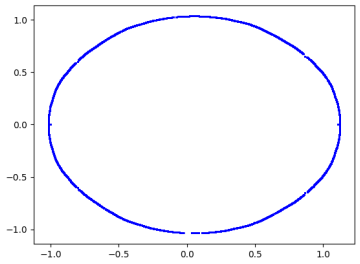

(b) = 0:1.

Experiment 5.1.2. The second experiment (see Figure 5.3), shows that the deformations and quantity of seemingly separated points increase monotonically in $j\ j$. We can also observe a qualitative di erence between the signs, whereas the structure contracts for positive values, it expands for negative values.
This is a strong indicator, that the reason for our counterintuitive results is the limited word length. The Mobius transformations we are using change continuous as we change , hence we are transforming the circle we were starting with continuously.

Figure 5.3: Values near zero.

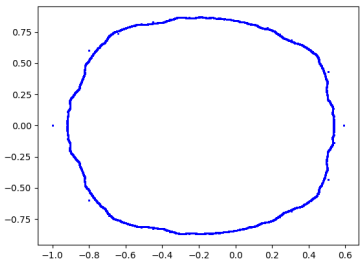

(a) = 0:5.

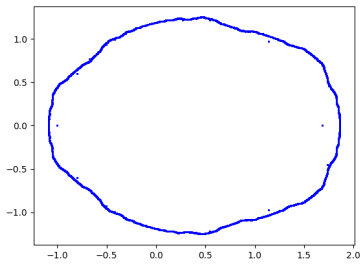

(b) = 0:5.

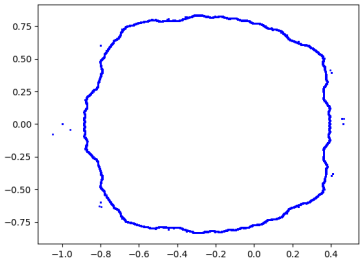

(c) = 0:7.

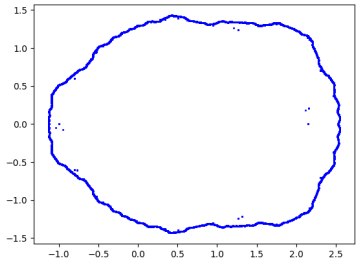

(d) = 0:7.

We should further investigate these seemingly separated points. As we zoom in on $1 + 0i$, we can see in Figure 5.4, that it is actually a cluster of points. This agrees with our previous theory and is an additional sign, that the limit set should fill the plane.

Figure 5.4: Zoom of $1 + 0i$, with $= 0.5$.

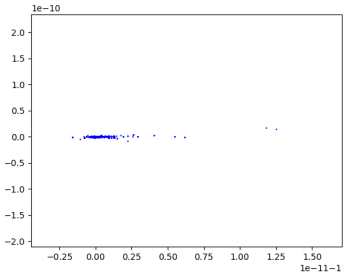

Experiment 5.1.3. In the third experiment, we only focused on positive values, but the results can be transferred analogously to the negative values. We will increase even further, to examine where this continuous change leads us.
We can observe in Figure 5.5, that for large enough the result is actually as chaotic as we thought it would be at the beginning.

Figure 5.5: Qualitative change.

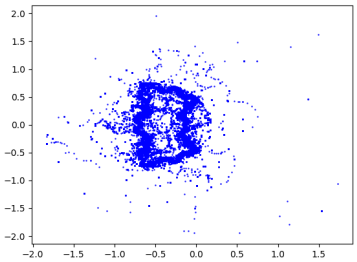

(a) $= 1.5$. (b) $= 1.6$.

Experiment 5.1.4. For our last experiment, we have chosen = =2, which corresponds to a quarter rotation. These values result in nice fractal structures, reminiscent of the Mandelbrot set or more in general terms Julia sets.

Figure 5.6: Discrete examples.

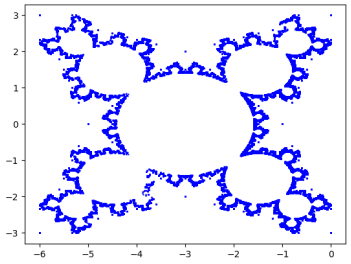

(a) = =2. (b) = =2.

The reason for this nice behavior is that the two generated groups G^+ and G are discrete, which can be shown as follows. The set,

$$\mathrm{Z}[i] := \{a + bi \in \mathrm{C} \mid a, b \in \mathrm{Z}\},$$

is a discrete subset of C and forms a ring, if equipped with the standard addition and multiplication of complex numbers. Hence, $GL_2(\mathrm{Z}[i])$ is discrete in $GL_2(\mathrm{C})$. The matrices $A' := e^{i\frac{}{2}}A$ and $B' := e^{i\frac{}{2}}B$ have coefficients in $\mathrm{Z}[i]$ and their determinant is an element of $\{1, i\}$, which can be shown by simple computations. Therefore, A', B' are both elements of $GL_2(\mathrm{Z}[i])$ and $G' := \langle A', B' \rangle$ is a subgroup of $GL_2(\mathrm{Z}[i])$. As a subgroup of a discrete group G' must be discrete in $\{A \in GL_2\mathrm{C} \mid det(A) \in \{1, i\}\}$. In $\mathrm{P}GL_2(\mathrm{C})$ G' and $\langle A, B \rangle$ are the same group, hence $\langle A, B \rangle$ is discrete in $\mathrm{P}GL_2(\mathrm{C})$, since discreteness in $\{A \in GL_2\mathrm{C} \mid det(A) \in \{1, i\}\}$ implies discreteness in $\mathrm{P}SL_2(\mathrm{C})$, the groups G^+ and G are discrete.

5.2 Gluing Angles

This section will introduce the gluing angles $\quad ; \quad 2 [\quad ; \quad)$, which allow us to add a rotation to our identi cations $A_{d;t}$ and $B_{d;s}$. Figure 5.7 shows how we want to implement this for the identi cation $A_{d;t}$ and the parameter . We want it to be a rotation around the shared edge of the two quadrilaterals Q and $A_{d;t}(Q)$.
The parameter will then describe a rotation around the shared edge of Q and $B_{d;s}(Q)$. We chose this rotation to be clockwise, so the signs of and the sign of the imaginary part of $B_{d;s}(Q)$ agree.

Figure 5.7: Gluing angle .

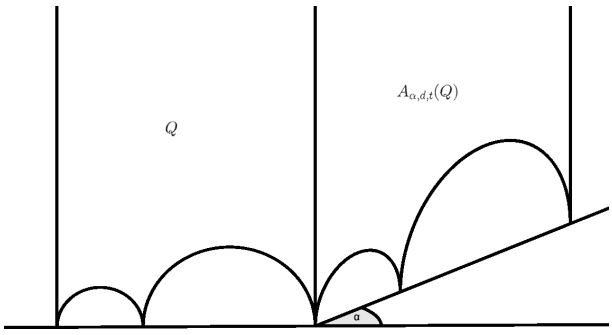

It is easily veri able that we can realize every gluing angle with our chosen parameters. We can now create our new isometries similarly to the identi - cations of the bent quadrilaterals, by combining $A_{d;t}$ and $B_{d;s}$ with rotations. Which leads to the following de nition:

De nition 5.2.1. Given the parameters $d;t;s \; 2$ R and $\quad ; \quad 2 [\quad ; \quad)$, the isometries $A \; _{;d;t}; B \; _{;d;s} \; 2 \; PSL_2(C)$, that identify the opposite sides of a quadrilateral as described above are given by the matrices

$$A \; _{;d;t} = \begin{pmatrix} e^{\frac{i}{2}} & e^{d}(e^{\frac{i}{2}} \quad e^{\frac{i}{2}}) \\ 0 & e^{\frac{i}{2}} \end{pmatrix} A_{d;t}; \; B \; _{;d;s} = \begin{pmatrix} e^{\frac{i}{2}} & e^{\frac{i}{2}} \quad e^{\frac{i}{2}} \\ 0 & e^{\frac{i}{2}} \end{pmatrix}^{!} B_{d;s}:$$

Because we already discussed the visualization process in H^3 in the last section, we go directly to the experiments. We will vary and set = . Due to the symmetry of this choice, it is su cient to focus on positive values for . In addition, we will again set $d = t = s = 0$, this has the consequence that the commutator $[A \; _{;d;t}; B \; _{;d;s}]$ is parabolic and has a xed point at 1. Therefore, $1 \; 2$ if the deformed group is discrete.
We will proceed similarly to the previous experiment, starting with values near zero, increasing the value till we get a qualitative change and then trying to nd values which create special patterns.

Experiment 5.2.1. The first experiment (see Figure 5.8) shows, that for values near zero the structure is still similar to a circle. In comparison to our bent quadrilateral experiments, the deformations are earlier noticeable. Additionally, we can see that there are no separated points. This suggests that the groups are still discrete when is small, which is consistent with our expectations.

Figure 5.8: = 0.05 and = 0.05.

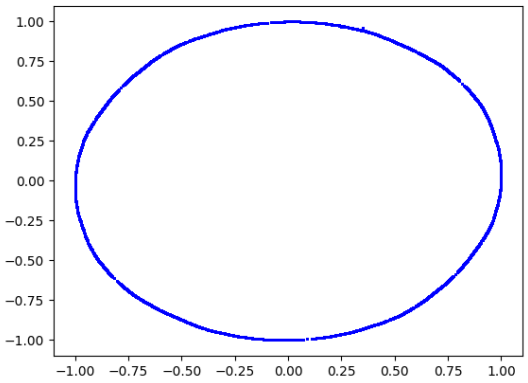

Experiment 5.2.2. In the second experiment, we can see the increasing deformations. The structures only vaguely resemble circles, but again there are no separated points. Even though the structures in Figure 5.9 look very different to the structure from the first experiment, we can not observe a qualitative change yet.

Figure 5.9: Increasing deformations.

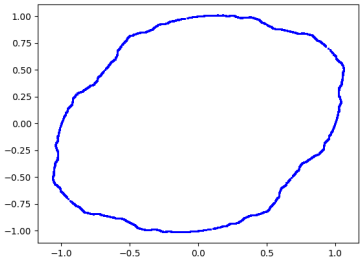

(a) = 0.4096 and = 0.4096.

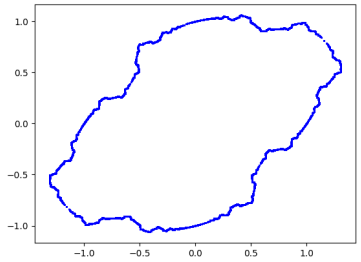

(b) = 0.8192 and = 0.8192.

As we can see in Figure 5.10, this is preserved even if we further increase to 1.5. However, the deformations become so large that the structure no longer

resembles a circle at all, but it is now very clear, that the limit sets are fractal curves.
The holes we can see in these curves are just a product of our physical limitations, if we could have words of in nite length or at least hundreds of letters, they would be lled.

Figure 5.10: Fractal curve.

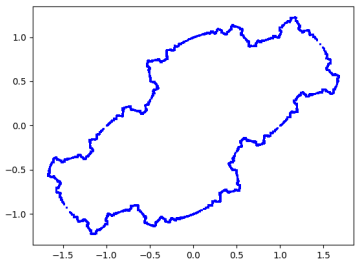

(a) = 1:2 and = 1:2.

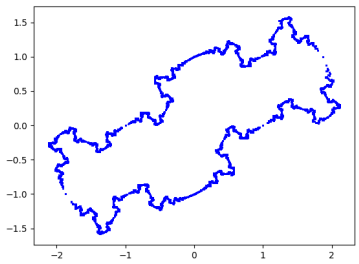

(b) = 1:5 and = 1:5.

Experiment 5.2.3. By increasing even further, we can nally provoke a qualitative change, the limit sets start to accumulate everywhere. This change takes place between 2 and 2:1, while the limit set for = 2 is still a very deformed circle, for = 2:1 it will correspond to the complete boundary of H^3. The described property of the limit sets might not be completely clear in Figure 5.11, but this is again just a consequence of our limitations in word length.

Figure 5.11: Qualitative change.

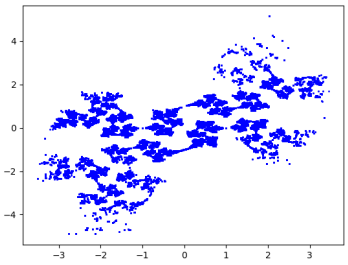

(a) = 2:0 and = 2:0.

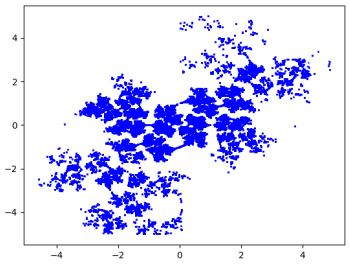

(b) = 2:1 and = 2:1.

When = 2:1, we can still identify some patterns in the limit set, similar to our experiments with small values. If we increase even further, the limit sets also become chaotic (see Figure 5.12).

Figure 5.12: Chaotic space filling sets.

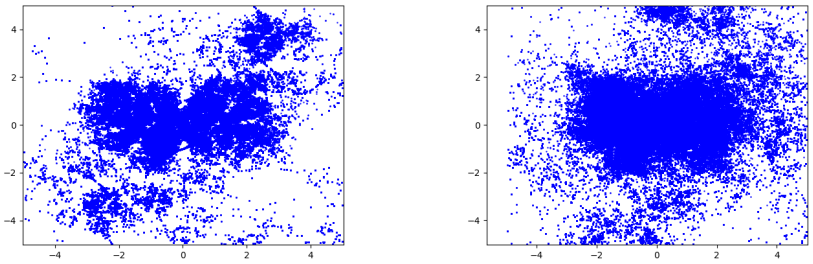

(a) = 2:3 and = 2:3. (b) = 2:5 and = 2:5.

Experiment 5.2.4. The special value we want to investigate in the last experiment is $2\pi/3$, the limit set (see Figure 5.13) seems similar to Figure 5.11b and indeed both are equal to $\partial\mathbb{H}^3$.
So, there is no difference between their limit sets, but there is a distinction in the generated groups. The group with $= 2\pi/3$ is discrete, whereas the groups with $> 2\pi/3$ are most likely not.
We can show the discreteness, similar to the last experiment of the previous section. First, we define $\omega := \pi/2 + i\sqrt{3}/2$ and note that $\mathbb{Z}[\omega]$ is a discrete subset of $\mathbb{C}$. Since $\mathbb{Z}[\omega]$ forms a ring, $PSL_2(\mathbb{Z}[\omega])$ is a discrete subgroup of $PSL_2(\mathbb{C})$. By simple computations we can prove, that $A_{2\pi/3;0;0}$ and $B_{2\pi/3;0;0}$ are elements of $PSL_2(\mathbb{Z}[\omega])$, which implies the discreteness of the generated group.

Figure 5.13: $= 2\pi/3$ and $= 2\pi/3$

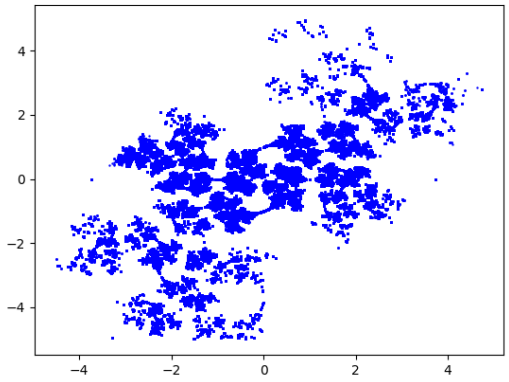

Bibliography

[Mil06] John Milnor. *Dynamics in one complex variable*. Princeton University Press, Princeton, NJ, 2006.

[Mar07] Albert Marden. *Outer circles*. Cambridge University Press, Cambridge, 2007.

[MSW15] David Mumford, Caroline Series, and David Wright. *Indra's pearls*. Cambridge University Press, Cambridge, 2015.

[Mar16] Bruno Martelli. *An Introduction to Geometric Topology*. CreateSpace Independent Publishing Platform, 2016.

[CM17] Matt Clay and Dan Margalit, eds. *Office hours with a geometric group theorist*. Princeton University Press, Princeton, NJ, 2017.